Two-Photon Photolysis of 2-Nitrobenzaldehyde Monitored by Fluorescent-Labeled Nanocapsules

Alberto Diaspro,*,† Federico Federici,† Cristiano Viappiani,‡ Silke Krol,† Marzia Pisciotta,† Giuseppe Chirico,§ Fabio Cannone,§ and Alessandra Gliozzi†

INFM, Department of Physics, University of Genoa, Italy, INFM, University of Parma, Italy, and INFM, University of Milan−Bicocca, Italy

Received: April 8, 2003; In Final Form: July 28, 2003

In this paper, we report, for the first time, experimental evidence of multiphoton photolysis of a caged proton compound, 2-nitrobenzaldehyde (*o*-NBA), using a new sensor system that utilizes fluorescent-labeled nanocapsules, i.e., a fluorescent nanostructured shell of micrometric size and nanometric thickness. The photolabile compound undergoes one-photon absorption in the UV range (200−380 nm), and the mechanism that leads to proton release is based on the well-known 2-nitrobenzyl photochemistry, which has been used for many photoactivatable-caged compounds. Because the use of UV excitation can cause biological damage, we changed our focus to multiphoton absorption−uncaging processes. The induced pH decrease was monitored by imaging changes in the pH-dependent emission of fluorescein isothiocyanate that was embedded in a nanostructured system (so-called "nanocapsules"). The nanocapsules with covalently bound dyes allow improved stability in fluorescence monitoring. Moreover, an original image processing method is introduced to quantify the uncaging. Using a femtosecond Ti:sapphire laser that was operating at 720 nm, with a pulse width of ∼200 fs at the sample, delivered through an adapted confocal laser scanning head and a 1-min exposure time with high power (45−50 mW), we obtained appreciable photolysis of 2-nitrobenzaldehyde. So far, we demonstrated that fluorescent-labeled nanocapsules are a suitable system as fluorescence sensors.

Introduction

The expanding interest in photoactivatable caged compounds for biological applications is leading, on one hand, to the development of new classes of caged effectors and photosensitive molecules and, on the other hand, to new experimental techniques for in vivo uncaging.

One of the largest classes of caged molecules that has been exploited so far is based on the photochemistry of 2-nitrobenzyl chromophores. This classification is comprised of an impressive number of caged effectors and photolabile parent compounds.[1,2] One of the crucial problems in the uncaging process is that the photolysis requires high-energy beams. The use of high-intensity UV excitation is sometimes not compatible with biological samples, because it causes damage; therefore, it is of the greatest interest to exploit the photolysis capabilities under two-photon and multiphoton excitation (TPE and MPE, respectively) using high-power, near-infrared femtosecond lasers.[3,4] MPE is an effective technique whose capability relies on nonlinear interactions between short (100 fs) laser pulses at a high repetition frequency (80 MHz) and the sample, which leads to the simultaneous absorption of two or more photons within the excitation process.[5,6]

Because of this nonlinear dependence on illumination intensity, fluorescence is expressed strictly in the vicinity of the focal plane, thus reducing out-of-focus effects, improving signal detection, and performing intrinsic optical sectioning.

Moreover, the use of longer wavelengths (with respect to single photon microscopy) couples a deeper penetration power with less overall phototoxicity, which makes this technique particularly useful in the presence of delicate targets such as biological samples.

Multiphoton (MP) uncaging for nitrophenyl-EGTA, which is one of the most popular caged Ca^{2+} compounds, has been shown to be scarcely efficient on the millisecond time scale, because of the low MP cross section of these chromophores.[7,8] Also, 4,5-dimethoxy-nitrophenyl-EGTA, which is obtained from nitrophenyl-EGTA via the addition of methoxy substituents at positions 4 and 5, proved to be functional for MP uncaging, also on a submillisecond time scale.[9] A compound that is based on a similar chromophore (a 2-nitrobenzyl system modified with methoxy functionalities at positions 4 and 5) but with lower uncaging yield, dimethoxy-nitrophen, was shown to be incapable of producing appreciable Ca^{2+} release on millisecond time scales.[7,8] The near-UV, $n\pi^*$ electronic transition of unmodified 2-nitrobenzyl-based caged compounds do not possess a sufficiently high TPE or MPE cross section to cause rapid (submillisecond) and extensive photolysis upon excitation in the near-infrared range of the laser powers used in the current experimental setups. However, it is of general interest to investigate the possibility of obtaining MP uncaging also under steady-state conditions, where dynamics is less important, whereas spatial localization of the uncaging process is crucial. Furthermore, a combination of MP cross section and photolysis yield is expected to control the effectiveness and speed of the uncaging.

A few compounds that function as caged protons capable of imposing rapid net acidification have been described previously. Among these is 2-hydroxyphenyl-1-(2-nitrophenyl)-ethyl phosphate.[10] More recently, a new caged proton compound, 1-(2-nitrophenyl)-ethyl sulfate, has been characterized that promises to be able to achieve large pH jumps in solution.[11] The

* Author to whom correspondence should be addressed. E-mail: diaspro@fisica.unige.it.
† University of Genoa.
‡ University of Parma.
§ University of Milan−Bicocca.

10.1021/jp034921i CCC: $25.00
Published on Web 09/12/2003

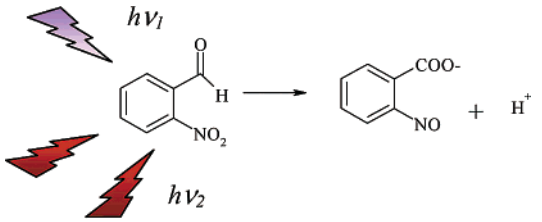

Figure 1. Photolysis scheme for *o*-NBA under the one-photon (violet) or two-photon (red) excitation ($\nu_1 \approx 2\nu_2$) regime.

photochemical rearrangement of 2-nitrobenzaldehydes to 2-nitrosobenzoic acids also has been used as a source of caged protons for the water-soluble derivative 4-formyl-6-methoxy-3-nitrophenoxyacetic acid.[12] Preliminary tests were performed on 2-nitrobenzaldehyde (*o*-NBA), which possesses the same photolabile chromophore as 2-nitrobenzyl-based caged compounds and, because of its photochemistry, can be used to increase the proton concentration rapidly in solution upon photoexcitation and, as such, functions as an efficient photoactivatable caged proton. This molecule absorbs in the near-UV range, with a weak electronic transition extending to ~380 nm, and its photochemistry,[13] as well as the possibility of using it as a photolabile caged proton,[14−16] have been previously established. NBA induces fast pH jumps in aqueous solutions in a series of investigations;[17−19] however, no attempt has been made so far to obtain proton release under the TPE or MPE regime using a near-infrared femtosecond laser.

Figure 1 shows the reaction scheme for the irreversible proton uncaging from NBA that leads to *o*-nitrosobenzoic acid. This process is completed in <5 ns.[13,14,19]

The advantage for proton-caging compounds is that pH changes are easy to detect. Coupling the MPE photolysis to TPE fluorescence imaging will allow in vivo investigations of processes that are triggered by the photoreleased effectors. However, one of the main problems that are encountered in the imaging of fluorescence intensity changes due to pH jumps is the fast diffusion of the free dyes in solution. Preliminary attempts performed in solutions that contain fluorescein isothiocyanate (FITC) and *o*-NBA molecules were affected by diffusion processes that mask actual pH local jumps and lead to poorly interpretable results (data not shown). It was thus necessary to develop a fluorescent system with immobilized dyes in solution. For this application, shells that were made of fuzzy nano-organized polyelectrolytes (named nanocapsules for their capability to control thickness at the nanometer scale) with dyes covalently bound to one or two capsule layers are revealed to be a type of pH sensor. Here, the amount of fluorescent dyes does not change or move while inducing the uncaging process. Therefore, a quantification of intensity variation by local pH jumps, which are unaffected by actual FITC fast-diffusion processes, is practical. Only acridine-containing polymers, which are highly sensitive and selective sensors for ferric ions, were reported by Lee[20] as another method to monitor fluorescence changes by means of a polyelectrolyte multilayer system. Fluorescence changes, in confocal and in near-field scanning optical systems, were also used for the detection of photo acid formation in studies related to the photo initiation of polymerization by photo acid formers.[21]

In this paper, we report some preliminary results on the two-photon photolysis of *o*-NBA, which leads to the release of protons within fluorescent-labeled polyelectrolyte capsules. The coupling of TPE with FITC-tagged nanocapsules is a key step for monitoring the local release of H^+ ions from *o*-NBA. To our knowledge, this is the first report of a multiphoton-induced decrease in pH using a photolabile compound. Previous studies showed the possibility of reducing the pH via the photolysis of 2-hydroxyphenyl-1-(2-nitro)-phenylethyl phosphate (NPE-caged phosphate) in a cellular system but with a pulsed UV laser.[10]

Materials and Methods

Materials. Fluorescently fuzzy nanostructured capsules, which are called nanocapsules, were constructed using polyelectrolytes and a fluorescent dye. Polyelectrolytes, poly(styrene sulfonate sodium salt) (PSS, with a molecular weight of MW = 70 000 Da) and poly(allylamine hydrochloride) (PAH, MW = 15 000 Da), as well as the pH-sensitive fluorescent dye fluorescein isothiocyanate (FITC), were obtained from Aldrich (Milan, Italy). PAH was labeled with FITC following a labeling protocol that has been described in detail elsewhere.[22,23] The removal of unbound FITC was performed by dialysis against Milli-Q-grade water or 0.5 M NaCl solution for at least one week by means of a dialysis membrane with a cutoff of 3.5 kDa (Spectrum Laboratory Products, Gardena, CA).

The chemicals used to prepare the calcium carbonate crystals (Na_2CO_3 (anhydrous), $MgCl_2 \cdot 6H_2O$, and $CaCl_2 \cdot 2H_2O$) were purchased from Sigma (Milan, Italy). All chemicals were utilized without further purification. Milli-Q-grade water (Millipore Corp., Bedford, MA) with a specific resistance of 18.2 MΩ/cm was used in all solutions and in the experimental and cleaning steps. The compound 2-nitrobenzaldehyde (*o*-NBA) was obtained from Sigma−Aldrich and was recrystallized from ethanol before use.

Methods. The preparation of the calcium carbonate crystals primarily followed the method that was described by Kitamura[24] and was based on the polymorphism between vaterite (spherical) and calcite (rhombohedric). The Na_2CO_3 solution (0.01 M) was added immediately and by hand to the $MgCl_2/CaCl_2$ solution in a common ultrasonic cleaner (model Transonic 130, ADAC Laboratories, Milpitas, CA) without stirring. The concentration of Ca^{2+} ions was equal to that of carbonate and the magnesium-to-calcium ratio was 1:4, which induced peanut-shaped templates 5−10 μm in size. These particles were subjected to continuous sonification for 5 min and then centrifuged and washed twice with pure water. Finally, they were completely dried at 50 °C in the oven and stored as a powder.

The nanocapsule preparation followed the layer-by-layer method that has been previously described in detail.[25,26] These capsules were called nanocapsules in the following discussion, because of their nanostructured capsule walls. Despite the size, which can vary from tens of nanometers to hundreds of micrometers, the thickness of nanocapsules can be controlled (within the nanometer scale), as well as their permeability.[22,26]

In the first step, charged calcium carbonate crystals suspended in a 0.5 M NaCl solution were coated via deposition of the polycation. The cores then were incubated for 5 min, after removal of the unbounded polyelectrolyte by centrifugation and two washing steps with 0.5 M saline; next, the polyanion PSS, which was treated in a similar manner, with a concentration of 2 mg/mL PE in 0.5 M NaCl solution, was added for 5 min to the coated crystals and, because of the charge inversion in the first step, were attached to the PAH layer. The first step then was repeated with a fluorescent-labeled PAH. The deposition of polyelectrolyte layers was repeated until the crystals were covered with six layers, two of which were fluorescent layers, by means of FITC−PAH. The decrease in the fluorescence intensity of FITC, because of pH changes, is well characterized[27] and was also stated by preliminary experiments (data not shown). The nanocapsules were used without dissolving the core and stored in 0.5 M NaCl before use.

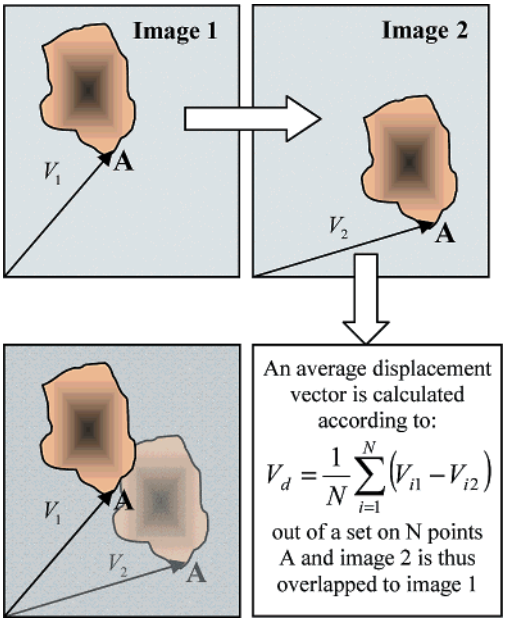

Figure 2. Scheme of the algorithm developed to overlap images for image analysis.

NBA was dissolved in Milli-Q-grade pure water, and the pH was set to 7 through the addition of proper volumes of NaOH and HCl solutions. The concentration was adjusted to obtain an absorbance of ~0.1 over a 1-cm optical path at 260 nm. Finally, the solution was mixed with an aqueous suspension (pH = 7) of FITC-labeled nanocapsules.

Image Acquisition and Analysis

A drop of sample was placed on a glass coverslip (nominal thickness of 0.17 mm) and imaged at 720 nm with a mode-locked Ti:sapphire infrared pulsed laser (model Tsunami 3960, Spectra Physics, Mountain View, CA) that was focused through a Nikon 1.3-NA 100× oil-immersion objective. The input power to the scanning head was ~20 mW (~7 mW on the focal plane) and a 535HQ (selective for fluorescein emission) was used as a barrier filter ahead of the photomultiplier tube (PMT) detectors.[28]

Within the 70 μm × 70 μm field of view previously imaged, a small region (13 μm × 13 μm) was chosen; this small area, which is described in the following, is called the uncaging spot. This area, which is in the direct neighborhood of the nanocapsules, was the focus point of the laser beam, and the region was scanned for ~1 min at high power (45−50 mW) and the laser acted on a neutral-density filter to induce uncaging of the protons. The power then was reduced to the commonly used 20 mW power that is used for scanning, and this region was imaged again. The nanocapsule that contained buffer solution without NBA served as a control, to reveal photobleaching effects or other experimental artifacts (such as *xy*-displacement or *z*-defocusing) that may be due to our laser-scanning device. Imaging conditions and parameters were maintained constant for each set of measurements.

Images were analyzed by first reducing background noise, through the application of a median filter (3 pixels in size). Furthermore, a spatial offset parameter was calculated to shift one region to another and to obtain a more precise overlapping between them. This algorithm, which was developed within Matlab (The Mathworks, Natick, MA), calculates an average center displacement vector of the manual setting of the corresponding points in the two images (Figure 2). After this alignment procedure, the image recorded after the uncaging was subtracted from the image that was recorded before the uncaging, and data analysis was performed on the pixel intensity of this difference array. The number of pixels that correspond to each possible intensity level is counted: positive levels account for a decrease of fluorescence emission from the sample whereas negative levels account for an increase of it. Background pixels whose intensity level is zero in both of the images are also counted separately, to exclude them from further statistical calculations. An estimate of the average intensity for each data acquisition is calculated, according to the following relationship in which background pixels are excluded:

$$\text{average value} = \sum_{s=1}^{256} s(n_s^+ - n_s^-)$$

where n_s^+ is the percentage of the pixels (in the difference array) whose intensity level is s and n_s^- is the percentage of the pixels (in the difference array) whose intensity level is $-s$.

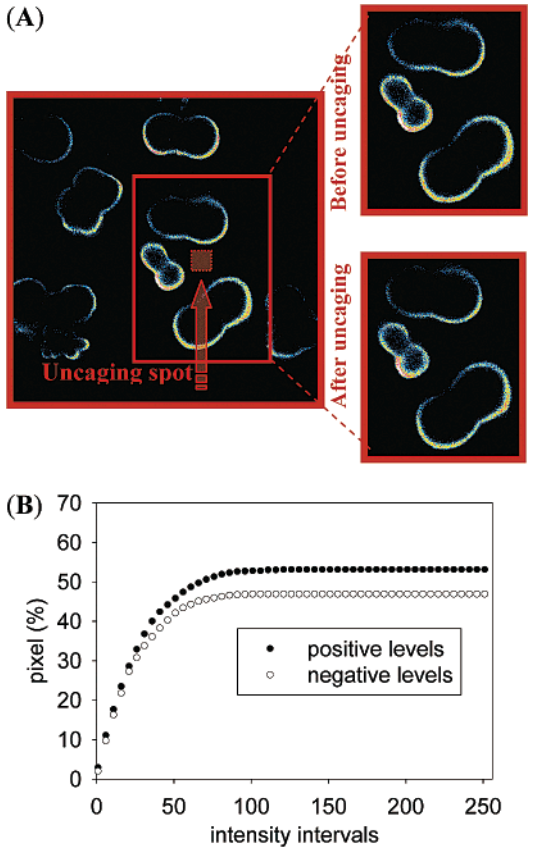

Figure 3. (A) Two-photon excitation images of FITC-doped polyelectrolyte nanocapsules ((PAH/PSS)$_3$, 3rd and 5th layer FITC-labeled). Fluorescein emission was excited at a wavelength of 720 nm, in the absence of 2-nitrobenzaldehyde, before (upper image, right row) and after (lower image, right row) high-energy scanning. (B) Image analysis showing the percentage of the number of pixels ((●) positive intensity level (decrease) and (○) negative intensity level (increase)) versus the number of intensity-level intervals, in the absence of NBA.

Results

The decrease in FITC intensity that is due to pH changes can be observed by comparing the TPE images before and after uncaging protons by photolysis for samples without NBA (Figure 3A) and more clearly for capsule suspensions that contain NBA in the buffer solution (Figure 4A). These results are supported by the image analysis presented in Figures 3B

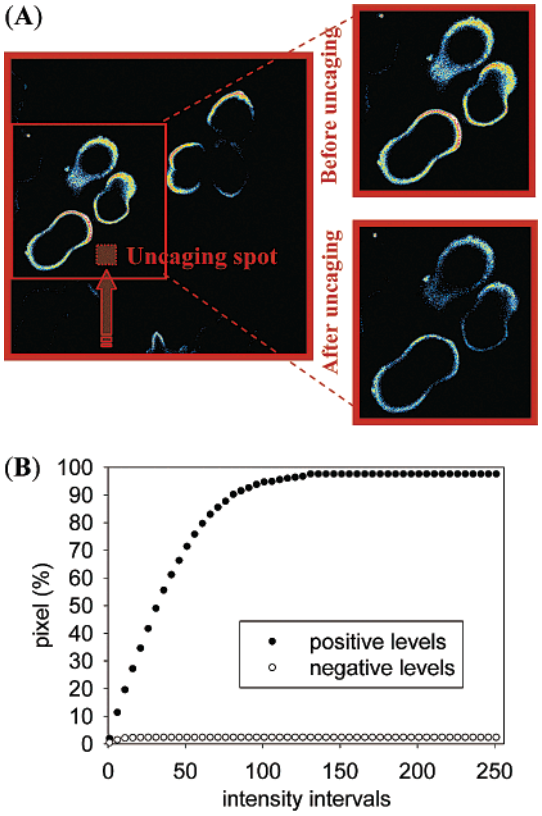

Figure 4. (A) Two-photon excitation images of FITC-doped polyelectrolyte nanocapsules ((PAH/PSS)$_3$, 3rd and 5th layer FITC-labeled). Fluorescein emission was excited at a wavelength of 720 nm, in the presence of 2-nitrobenzaldehyde, before (upper image, right row) and after (lower image, right row) 2-nitrobenzaldehyde photolysis that was induced by high-energy scanning with multiphoton excitation at 720 nm. (B) Image analysis showing the percentage of the number of pixels ((●) positive intensity level (decrease) and (○) negative intensity level (increase)) versus the number of intensity-level intervals, in the presence of NBA.

and 4B, where positive and negative intensity intervals are plotted versus the percentage of pixels whose intensity values fall inside the considered interval. In the absence of NBA, the pixel intensities in the difference image are distributed fairly equally over each positive/negative intensity interval, whereas, in the presence of NBA, most of the pixels have a positive intensity level, which is expected for H^+ uncaging in a FITC-loaded nanocapsule solution.

The results show that, when high-powered scanning is conducted without NBA in the solution, this procedure does not lead to a significant change in the image average intensity: the percentage of positive intensity pixels in the difference array is approximately the same as, although slightly smaller than, the percentage of negative intensity pixels (see Figure 3B). The fact that the percentage of pixels with a positive intensity value is always bigger than that of pixels with a negative intensity value is consistent with a certain intrinsic decrease of fluorescence in both cases (with or without NBA), because of photobleaching effects. This finding shows that photobleaching effects on fluorescein represent only a minor contribution to the observed decrease in fluorescence emission when the sample also contains NBA. Therefore, the latter effect can be correlated with the photolysis of the *o*-nitrobenzyl compound and the release of protons to the solution. The data sets reveal that the overall fluorescence decrease is 4−5 times stronger when NBA is present in the nanocapsules solution (see Figure 4B). In Table 1, the results of a typical image analysis are listed. Each row is

TABLE 1: Statistics Performed over the Difference Array, Listed on Each Row for Every Single Data Acquisition[a]

	Percentage of Pixels		average intensity difference (a.u.)[b]
	positive level	negative level	
	With NBA		
sample 1	84	15	20
sample 2	84	15	31
sample 3	75	24	19
sample 4	97	2	36
sample 5	61	38	18
sample 6	66	33	13
sample 7	76	23	15
sample 8	77	22	18
			21
	Without NBA		
sample 1	57	41	5
sample 2	55	42	3
sample 3	52	47	2
sample 4	48	50	0
sample 5	58	40	8
			4

[a] The upper portion of the table refers to different data sets from separate uncaging experiments in the presence of 2-nitrobenzaldehyde (*o*-NBA) and, therefore, a pH decrease. The lower portion of the table shows data sets derived from control experiments in the absence of NBA. [b] Value given in boldface type represents the average value of the set of data that is presented.

related to the statistics that have been performed over the difference array of a single data acquisition. In the top portion of the table (the first eight rows of data), the table reports data from eight data sets that have been derived from separate uncaging experiments. The bottom portion of the table (the next five rows of data) show data sets that have been derived from separate experiments in the absence of NBA.

Note that if any artifact is involved in these results (such as defocusing or photobleaching effects), it should affect both experiments, in the presence and the absence of NBA. Therefore, we can exclude systematic effects of the data acquisition method on fluorescein emission. Hence, the observed decrease in FITC fluorescence emission is related to the multiphoton-induced H^+ uncaging from NBA, which leads to a pH decrease in the surrounding solution. Note that the local decrease of pH, and, thus, that of fluorescence, could be larger than we were able to observe. So far, we have been able to evaluate changes in the overall fluorescence emission only after a 1-min two-photon photolysis has been completed, because we cannot image the sample while the uncaging process is underway. It is reasonable to expect that, while high-power laser scanning is performed, photoreleased protons partially leave the focal volume in the microsecond and millisecond time scale, because of diffusion processes.[7,15]

To resolve this fast kinetic phase, it is necessary to achieve a substantial improvement in the switch between high-power scanning and fluorescence images acquisition after the high-power photolysis is finished.[7,9] This finding is of specific relevance if in vivo multiphoton photolysis is used to investigate, for instance, Ca^{2+} dynamics in a particular portion of the sample.

Our intent is now to gain better control of these phenomena by determining the extent to which the multiphoton uncaging process is dependent on the choice of wavelength and high scanning power. It will be also possible to have some important insights about the behavior of other photolabile compounds with several caged effectors, some of which present a reversible uncaging process. This phenomenon will eventually allow us to be capable of controlling the pH of the buffer by means of a photoreaction.

Substantial improvements in the photolysis rate are expected to occur through the use of a photosensitive chromophore, for instance, the 4,5-dimethoxy derivative of 2-nitrobenzaldehyde. Although the addition of methoxy substituents is known to reduce the photochemical yield of the reaction, an enhancement of the two-photon cross section in the near-infrared range is expected to occur,[9] which, hopefully, more than compensates for the decrease in efficiency.

Acknowledgment. Research performed under EU Nanocapsule (Grant No. HPRN-CT-2000-00159) and INFM PAIS UNCAGE2 grants.

References and Notes

(1) Marriott, G. In *Methods in Enzymology*; Academic Press: New York, London, 1998.

(2) McCray, J. A.; Trentham, D. R. *Annu. Rev. Biophys. Biophys. Chem.* **1989**, *18*, 239−270.

(3) Denk, W.; Piston, D.; Webb, W. W. In *Handbook of Confocal Microscopy*; Pawley, J. B., Ed.; Plenum: New York, 1995; 445−457.

(4) Callis, P. R. *Annu. Rev. Phys. Chem.* **1997**, *48*, 271−297.

(5) Denk, W.; Strickler, J. H.; Webb, W. W. *Science* **1990**, *248*, 73−76.

(6) Diaspro, A., Ed.; *Confocal and Two-Photon Microscopy: Foundations, Applications, and Advances*; Wiley−Liss: New York, 2002.

(7) Brown, E. B.; Adams, S. R.; Shear, J. B.; Tsien, R. Y.; Webb, W. W. *Biophys. J.* **1999**, *76*, 489−499.

(8) Brown, E. B.; Webb, W. W. *Caged Compounds*; Marriott, G., Ed.; Methods of Enzymology, Vol. 291; Academic Press: San Diego, CA, 1998.

(9) DelPrincipe, F.; Egger, M.; Ellis-Davies, G. C. R.; Niggli, E. *Cell Calcium* **1999**, *25*, 85−91.

(10) Khan, S.; Castellano, F.; Spudich, J. L.; McCray, J. A.; Goody, R. S.; Reid, G. P.; Trentham, D. R. *Biophys. J.* **1993**, *65*, 2368−2382.

(11) Barth, A.; Corrie, J. T. *Biophys. J.* **2002**, *83*, 2864−2871.

(12) Janko, K.; Reichert, J. *Biochim. Biophys. Acta* **1987**, *905*, 409−416.

(13) George, M. V.; Scaiano, J. C. *J. Phys. Chem.* **1980**, *84*, 492−495.

(14) Bonetti, G.; Vecli, A.; Viappiani, C. *Chem. Phys. Lett.* **1997**, *269*, 268−273.

(15) Viappiani, C.; Abbruzzetti, S.; Small, J. R.; Libertini, L. J.; Small, E. W. *Biophys. Chem.* **1998**, *73*, 13−22.

(16) Viappiani, C.; Bonetti, G.; Carcelli, M.; Ferrari, F.; Sternieri, A. *Rev. Sci. Instrum.* **1998**, *69*, 270−276

(17) Abbruzzetti, S.; Crema, E.; Masino, L.; Vecli, A.; Viappiani, C.; Small, J. R.; Libertini, L. J.; Small, E. W. *Biophys. J.* **2000**, *78*, 405−415.

(18) Abbruzzetti, S.; Viappiani, C.; Small, J. R.; Libertini, L. J.; Small, E. W. *Biophys. J.* **2000**, *79*, 2714−2721.

(19) Abbruzzetti, S.; Viappiani, C.; Small, J. R.; Libertini, L. J.; Small, E. W. *J. Am. Chem. Soc.* **2001**, *123*, 6649−6653.

(20) Lee, T. S.; Park, W. H.; Yang, C. D. *Macromol. Rapid Commun.* **2000**, *21*, 951−955.

(21) Catry, C.; Jeuris, K.; Jackers, C.; Hofkens, J.; Bastin, L.; Gensch, T.; Grim, P. C. M.; De Schryver, F. C.; Van Damme, M. *Langmuir* **1999**, *15*, 1364−1372.

(22) Donath, E.; Caruso, F.; Davis, S. A.; Möhwald, H.; Sukhorukov, G. B. *Angew. Chem., Int. Ed.* **1998**, *16*, 2202−2205.

(23) Sukhorukov, G. B.; Donath, E.; Knippel, E.; Knippel, M.; Lichtenfeld, H.; Möhwald, H. *Colloids Surf. A* **1998**, *137*, 253.

(24) Kitamura, M. *J. Colloid Interface Sci.* **2001**, *236*, 318.

(25) Decher, G. *Science* **1997**, *277*, 1232.

(26) Möhwald, H. *Colloids Surf. A* **2000**, *171*, 25.

(27) Haughland, R. P. *Handbook of Fluorescent Probes and Research Chemicals*, 6th ed.; Molecular Probes, Inc.: Eugene, OR, 1996.

(28) Diaspro, A.; Corosu, M.; Ramoino, P.; Robello, M. *Microsc. Res. Tech.* **1999**, *47*, 196−205.